Nematic DNA Thermotropic Liquid Crystals with Photoresponsive Mechanical Properties

Zhang, Lei; Maity, Sourav; Liu, Kai; Liu, Qing; Göstl, Robert; Portale, Giuseppe; Roos, Wouter H; Herrmann, Andreas

Link to publication in University of Groningen/UMCG research database

**ADVANCED
SCIENCE NEWS**
www.advancedsciencenews.com

NANO MICRO
small

Photomechanics

Nematic DNA Thermotropic Liquid Crystals with Photoresponsive Mechanical Properties

Lei Zhang, Sourav Maity, Kai Liu,* Qing Liu, Robert Göstl, Giuseppe Portale, Wouter H. Roos, and Andreas Herrmann*

Over the last decades, water-based lyotropic liquid crystals of nucleic acids have been extensively investigated because of their important role in biology. Alongside, solvent-free thermotropic liquid crystals (TLCs) from DNA are gaining great interest, owing to their relevance to DNA-inspired optoelectronic applications. Up to now, however, only the smectic phase of DNA TLCs has been reported. The development of new mesophases including nematic, hexagonal, and cubic structures for DNA TLCs remains a significant challenge, which thus limits their technological applications considerably. In this work, a new type of DNA TLC that is formed by electrostatic complexation of anionic oligonucleotides and cationic surfactants containing an azobenzene (AZO) moiety is demonstrated. DNA–AZO complexes form a stable nematic mesophase over a temperature range from −7 to 110 °C and retain double-stranded DNA structure at ambient temperature. Photoisomerization of the AZO moieties from the E- to the Z-form alters the stiffness of the DNA–AZO hybrid materials opening a pathway toward the development of DNA TLCs as stimuli-responsive biomaterials.

L. Zhang, Prof. K. Liu
State Key Laboratory of Rare Earth Resource Utilization
Changchun Institute of Applied Chemistry
Chinese Academy of Sciences
130022 Changchun, China
E-mail: kai.liu@ciac.ac.cn

L. Zhang, Dr. S. Maity, Q. Liu, Prof. G. Portale,
Prof. W. H. Roos, Prof. A. Herrmann[+]
Zernike Institute for Advanced Materials
Nijenborgh 4, 9747 AG Groningen, The Netherlands
E-mail: a.herrmann@rug.nl

L. Zhang
Key Laboratory of Sensor Analysis of Tumor Marker
Ministry of Education
College of Chemistry and Molecular Engineering
Qingdao University of Science and Technology
266042 Qingdao, China

Dr. R. Göstl
DWI-Leibniz Institute for Interactive Materials
Forckenbeckstr. 50, 52056 Aachen, Germany

[+]Present addresses: DWI-Leibniz Institute for Interactive Materials, Forckenbeckstr. 50, 52056 Aachen, Germany and Institute of Technical and Macromolecular Chemistry, RWTH Aachen University, Worringerweg 2, 52074 Aachen, Germany

1. Introduction

Lyotropic liquid crystals (LLCs) of DNA obtained by supramolecular self-assembly have attracted considerable attention as these condensed DNA mesophases have broad biological and biotechnological significance in an aqueous environment.[1–7] A variety of LLC structures ranging from nematic phases, over smectic and hexagonal states to cubic phases based on pristine DNA[8–15] and DNA-surfactant complexes[16–28] have been obtained by tuning DNA concentration, molecular weight, and surfactant type. These seminal findings enabled the development of powerful tools for drug delivery and gene therapy applications.[29–32] Although most investigations of DNA LCs are currently limited to aqueous solutions, research examining anhydrous DNA thermotropic liquid crystals (TLCs) is gaining momentum[33] owing to its relevance in DNA-based optoelectronic applications.[34–37] Recently, for example, a new class of smectic DNA TLCs has been generated by electrostatic complexation of single stranded (ss) oligonucleotides with surfactants containing two flexible alkyl chains.[38,39] Based on this type of DNA TLCs, an electrochromic device that exhibits a clock function and a ceiling temperature indicator was fabricated.[40] Despite these advances it is imperative to enrich ordered mesophases of DNA TLC materials with a greater degree of tunability

and control over their electrical, optical, and mechanical properties as well as to retain the double-stranded (ds) conformation of DNA in DNA-TLCs.

Light can be dosed with spatial, temporal, and energetic control and hence can be regarded as the optimal physicochemical stimulus to manipulate the properties of TLCs.[41,42] Consequently, there has been widespread and persistent interest in the development of photoresponsive TLC polymers exploiting the characteristics of photoisomerization and photoalignment.[43,44] For example, with the introduction of photochromic azobenzene units into TLCs, molecular switching events can be transmitted and amplified from the molecular to the macroscopic level in the form of mechanical work.[45] Hence, this opens an attractive route to realize actuator,[46,47] plastic motor,[45,48] shape memory,[49,50] and solar-energy harvesting systems.[51] To implement these attractive features of TLC polymers into a biological context, there is considerable demand for the development of TLC systems based on biomacromolecular architectures with photoresponsive mechanical properties[52–54] for the fabrication of smart soft biomaterials utilized as artificial skin and muscles.

Here we report a new class of DNA TLC materials exhibiting nematic mesophases whose mechanical behaviors can be controlled conveniently by irradiation with light. Since DNA TLCs exhibit remarkable mechanical properties,[38] we reasoned that modulation of these characteristics by the means of light-irradiation would add an unprecedented level of control over this type of material. Nematic DNA TLCs were prepared by electrostatic complexation of double- and single-stranded oligonucleotides with cationic surfactants containing two aliphatic chains and one aromatic azobenzene moiety (AZO) followed by dehydration. The light-induced *E*- to *Z*-isomerization proceeds smoothly in these solvent-free DNA–AZO complexes and grants access to photocontrol over their mechanical performance in case of double stranded DNA.

2. Results and Discussion

Initially, we synthesized a new cationic surfactant containing a quaternary ammonium group and two hydrophobic alkyl chains that are separated by a benzoic acid unit and an azobenzene moiety (AZO) through a four-step route (**Scheme 1**, experimental details and characterization are presented in the Supporting Information). In brief, the hydroxy group in position 4 of the *β*-resorcylic acid derivative **1** was reacted with bromobutane to yield the ether **2**. Subsequently, the second hydroxyl group in position 2 was also converted into the corresponding ether by employing 1,4-dibromobutane to yield compound **3**. The quaternary ammonium compound **4** was obtained by employing trimethylamine. In a transesterification reaction, 4-((4-octylphenyl)diazenyl)-phenol was introduced to furnish the azobenzene containing surfactant **5** (AZO) exhibiting branched alkyl chains.

Afterward, the photoisomerization behavior of the AZO surfactant was investigated employing UV–vis absorption spectroscopy during irradiation with UV-light (**Figure 1**A). Before UV-irradiation, the azobenzene exists predominantly in the *E*-form characteristically indicated by the π–π* transition at ≈330 nm.[41,55] We attribute the absorption band with a maximum at about 260 nm to the π-conjugated benzene rings present in both isomers. Upon UV-irradiation at 365 nm, the absorption intensity of the π–π* transition at around 330 nm decreased and the n–π* absorption peak at ≈434 nm increased indicating successful *E*- to *Z*-photoisomerization of the AZO surfactant. Based on the time-dependent UV–vis absorption spectra, an *E*- to *Z*-isomerization efficiency of at least 84% was determined in the AZO surfactant, which is in agreement with the analysis of proton nuclear magnetic resonance spectroscopy (¹H-NMR) (Figure S7, Supporting Information). After the exposure to visible light (450 nm,), the azobenzene could not be transformed back fully to the original *E*-form (Figure S8, Supporting Information). Due to the absence of an isosbestic point over the course of the
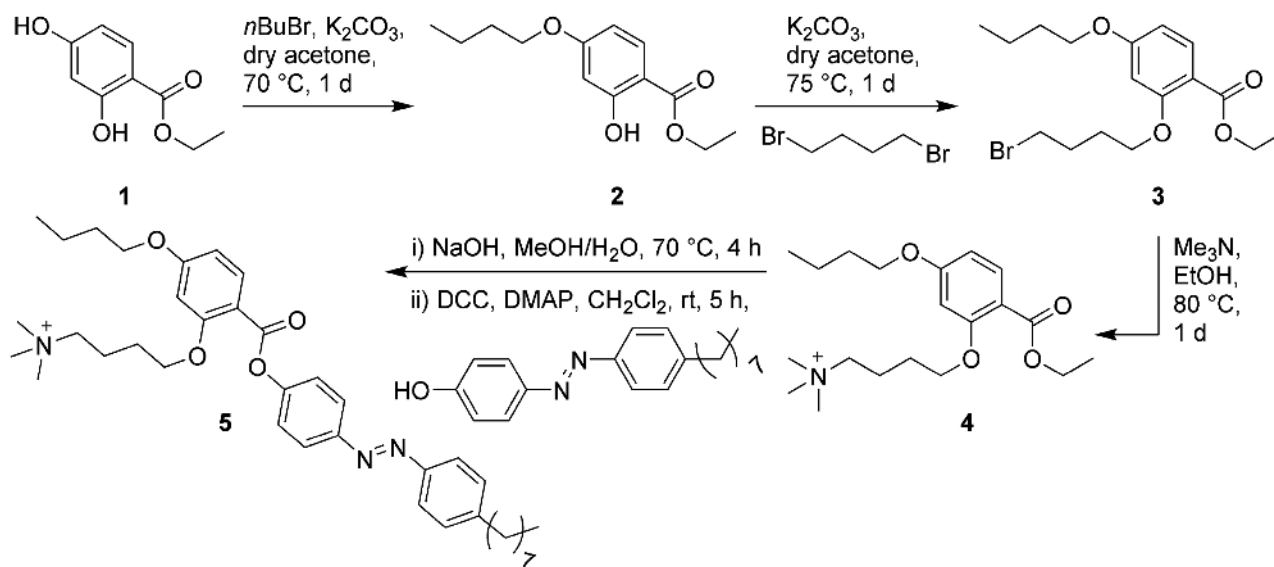
Scheme 1. The synthesis route of the cationic surfactant (AZO) containing a quaternary ammonium group, two hydrophobic alkyl chains, and two aromatic units including an azobenzene moiety.
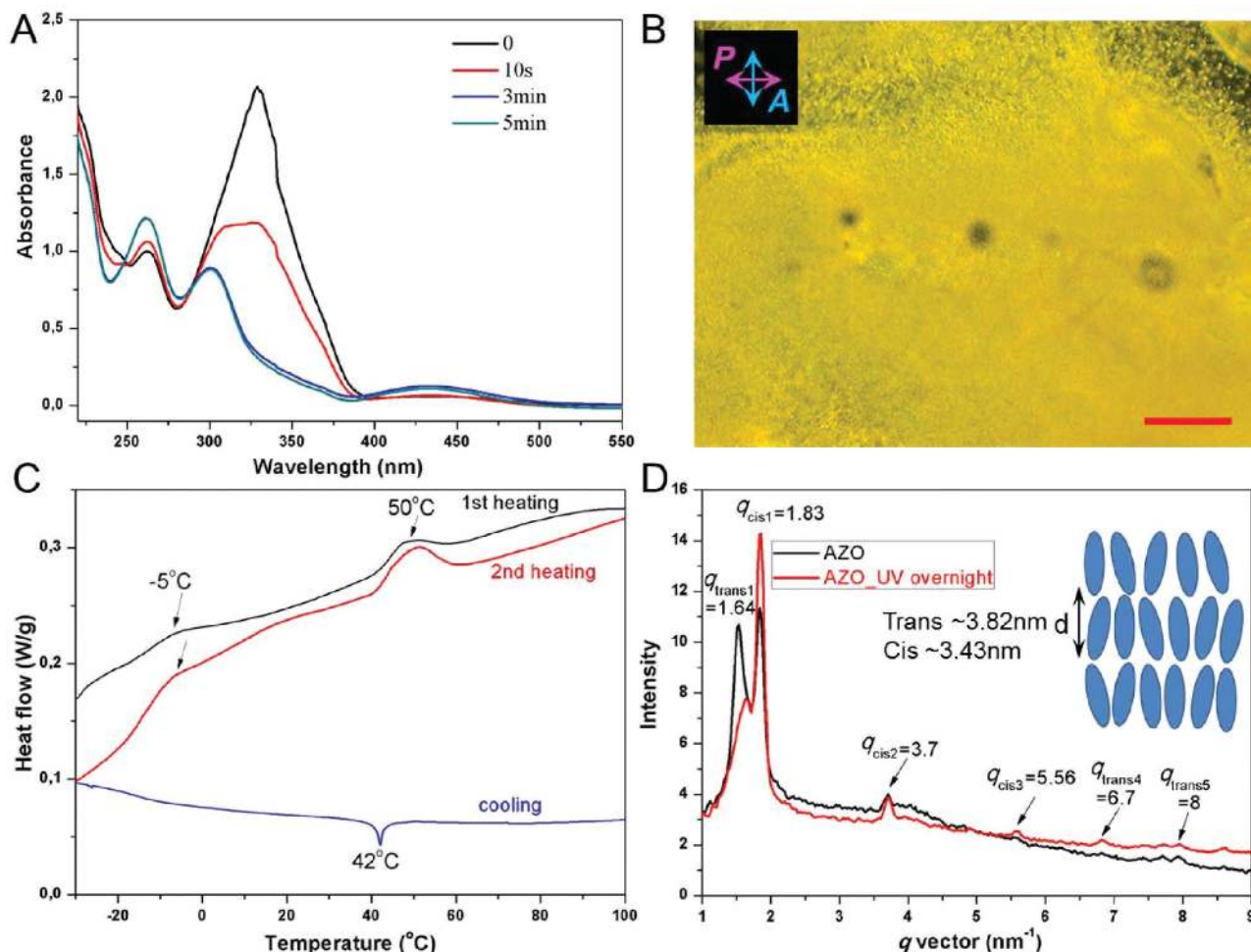
Figure 1. Characterization of the pristine AZO surfactant. A) UV–vis absorption spectra of the AZO surfactant in aqueous solution over the course of irradiation with UV-light accompanied by E- to Z-isomerization (concentration 65×10^{-6} M). B) POM image of the birefringent AZO surfactant at room temperature. Scale bar is 100 µm. C) DSC traces with phase transition temperatures of the AZO surfactant (at a heating/cooling rate of 5 °C min^{-1}). Two endothermic peaks at −5 and 50 °C indicate the crystalline-LC and LC-isotropic transitions of the AZO surfactant. D) SAXS profiles of the AZO surfactant recorded before and after the application of UV irradiation. The sharp first-order reflection peaks of E- and Z-isomers and their following harmonics are characteristic of long-range ordered lamellar structures of the AZO surfactant. The inset represents the molecular packing model of the surfactant. Isomerization of the AZO samples was performed employing a UV-lamp (0.5 mW cm^{-2}) at $\lambda_{exc} = 365$ nm.

irradiation, we attribute this effect to unspecific photodegradation of the AZO surfactant due to prolonged light exposure under aerated conditions.

Further characterization of the pristine surfactant was conducted by polarized optical microscopy (POM) analysis revealing that the lyophilized AZO surfactant is birefringent (Figure 1B), highly viscous, and has a TLC phase at room temperature. Differential scanning calorimetry (DSC) unraveled two endothermic peaks at −5 and 50 °C corresponding to the crystalline-LC and LC-isotropic transitions, respectively (Figure 1C). The ordered structural features of the pristine AZO surfactant were analyzed by small-angle X-ray scattering (SAXS). In the AZO mesophase, the sharp first-order reflection peaks of E- and Z-isomers and their following harmonics are characteristic of long-range ordered lamellar structures (Figure 1D, black curve). Based on the analysis of the two sharp first order reflection peaks at $q = 1.64$ nm^{-1} and $q = 1.83$ nm^{-1} ($d = 2\pi/q_1$), the smectic layer spacing of the two isomers can be determined

to 3.82 nm for the E- and 3.43 nm for the Z-isomer, respectively, approximately corresponding to the molecular dimensions of the AZO isomers. We note that the layer spacing difference of ≈0.39 nm of the two isomers also corresponds to the length change of about 0.35 nm from E- to Z-azobenzene.[56,57] Moreover, after irradiation with UV-light overnight, the sample was remeasured by SAXS at room temperature. We found that the intensity of the first-order diffraction of E-AZO decreased significantly and the diffraction peak of Z-AZO was increased (Figure 1D, red curve) clearly indicating that the E- to Z-isomerization of azobenzene can be performed successfully in the liquid crystalline phase. It should be noted, however, that unspecific photodegradation of the AZO molecule cannot be excluded fully because of UV exposure overnight. Conversely, after irradiation with 450 nm light for 24 h, the Z- to E-isomerization could not be observed in the AZO LC material. Packing effects may be responsible for this irreversible photoisomerization behavior in the AZO LC phase as the
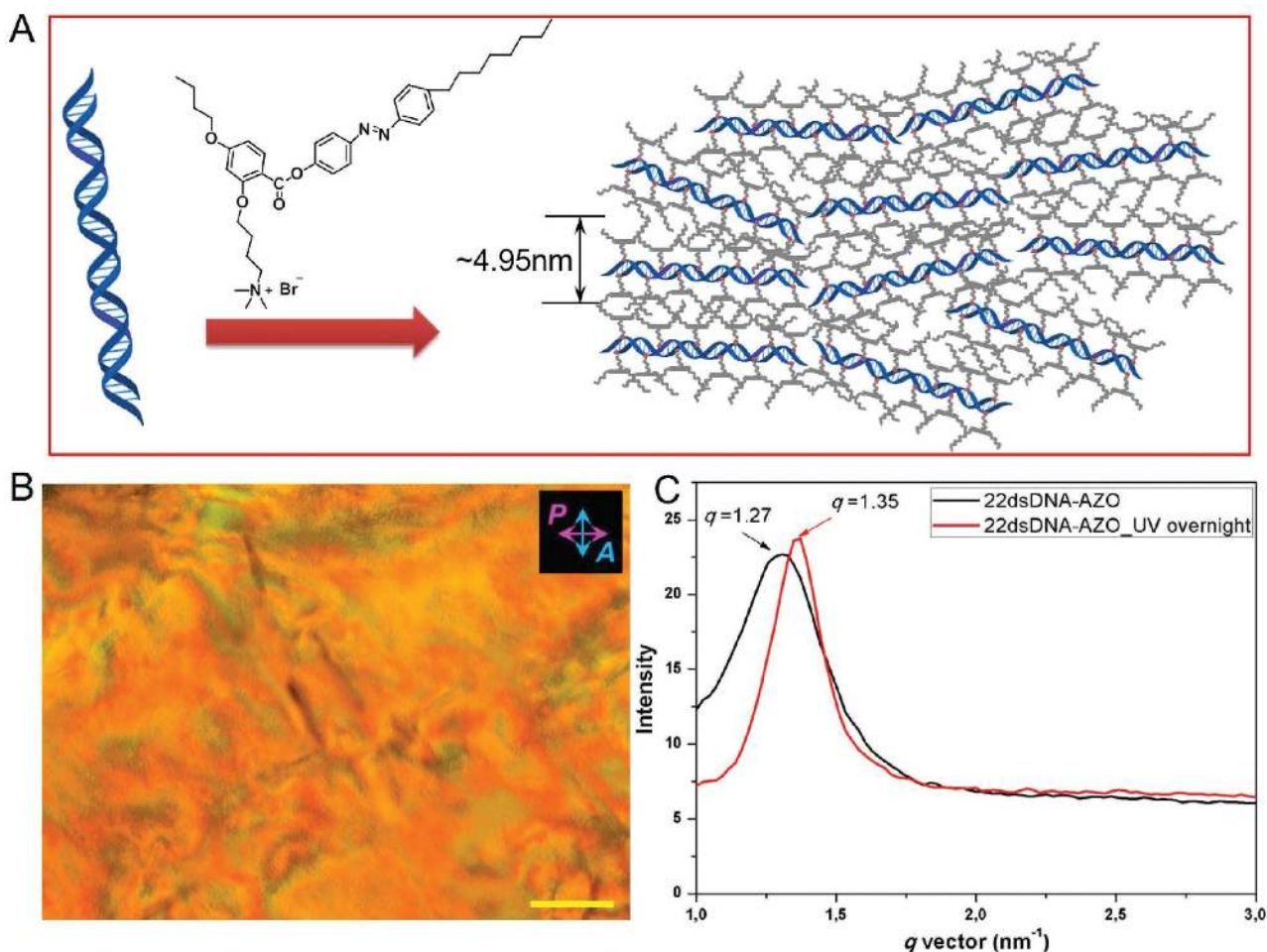
Figure 2. Preparation and characterization of the dsDNA–AZO nematic liquid crystals. A) The dsDNA–AZO nematic TLC material is formed by electrostatic complexation of double-stranded 22mer oligonucleotides and AZO surfactants. B) POM image of the dsDNA–AZO complex at room temperature showing typical schlieren textures characteristic of a nematic mesophase. Scale bar is 100 µm. C) SAXS profiles of the dsDNA–AZO complex (25 °C) recorded before and after the application of UV-irradiation. Two broad diffraction peaks corresponding to the *d* spacing of 4.95 and 4.65 nm indicate the *E*- to *Z*-isomerization of the azobenzene moiety in the nematic TLC material. Isomerization of the dsDNA–AZO samples was performed employing a UV-lamp (0.5 mW cm^{-2}) at λ_{exc} = 365 nm.

isomerization process is accompanied by a considerable geometrical rearrangement.[58]

Subsequently, a 22mer single stranded oligonucleotide and its complementary sequence were synthesized by conventional solid-phase synthesis.[59] The purity and molecular weight were confirmed by polyacrylamide gel electrophoresis and matrix-assisted laser desorption/ionization time-of-flight mass spectrometry (MALDI-TOF MS), respectively (Figure S9, Supporting Information). Mixing of an aqueous solution of 22mer dsDNA with cationic surfactants (AZO) results in precipitation of the dsDNA–AZO complex, which is then obtained in pure form after centrifugation and lyophilization (**Figure 2**A). Quantitative component determination of the dsDNA–AZO complex was carried out by NMR (Figure S10, Supporting Information) revealing the stoichiometry of the 22mer dsDNA and the AZO surfactants to be 1:52 (i.e., ≈1.2 AZO surfactant molecules per phosphate of the oligonucleotide). This indicates that a small number of extra surfactant molecules are present in the complex, which we attribute to the π–π and alkyl chain interactions among the AZO surfactants. Thermogravimetric analysis (TGA) of

the dsDNA–AZO sample revealed a water content of less than 5 wt% and also demonstrated the thermal integrity of the complex up to 200 °C. Above this temperature, decomposition starts (Figure S11, Supporting Information). At room temperature, the dsDNA–AZO material is soft and can be pressed. Birefringence with typical schlieren textures is observed (Figure 2B) indicating the formation of a nematic TLC phase in the dsDNA–AZO complex. Temperature-dependent POM analysis showed that the birefringent nematic textures melt away completely above 110 °C leaving only transparent isotropic liquid (Figure S12, Supporting Information). DSC results showed one broad endothermic peak from 45 to 120 °C in the virgin heating cycle, which may correspond to thermal dehybridization of dsDNA in the TLC material (Figure S13, Supporting Information). Additionally, a phase transition from crystal to LC was observed at around –7 °C.

Moreover, the ordered nematic features of the dsDNA–AZO TLC were analyzed by SAXS revealing a broad diffraction peak corresponding to the *d* spacing of 4.95 nm (Figure 2C, black curve). Besides the use of dsDNA, nematic

TLCs from ssDNA were fabricated (Figures S14 and S15, Supporting Information) and SAXS data indicate a nematic mesophase with a diffraction spacing of 4.5 nm for this LC complex. We attribute these values to the average diameter of the DNA–surfactant complexes that are composed of DNA units of 1–2 nm thickness and AZO surfactant molecules of 3–4 nm thickness. It should be noted that this average diameter of the ssDNA–AZO complex was only 0.55 nm smaller than the one of the mesophase formed by dsDNA–AZO, which is less than the diameter difference ($\approx$1 nm) of ssDNA and dsDNA.[60,61] We ascribe this difference to partial denaturation of the double stranded DNA in the solvent-free dsDNA–AZO mesophase. Additionally, the DNA–AZO TLC materials were characterized by SAXS after UV-irradiation (Figure 2C, red curve; Figure S14B, red curve, Supporting Information). We found that the diffraction spacing decreased hinting toward a successful *E*- to *Z*-isomerization in the TLC materials. However, unspecific photodegradation of the AZO molecule may contribute to this decrease because of overnight UV exposure. The most important result of the structural analysis is that the electrostatic assembly of anionic DNA and cationic AZO induces rearrangement of the AZO molecules from an originally lamellar phase in the pristine AZO surfactant (Figure 1) to a nematic mesophase in the DNA–AZO complexes.

In order to study the mechanical properties of the TLC materials, we subjected them to dynamic mechanical analysis employing a shear rheometer. We determined storage moduli (*G'*) representing the elastic portion and loss moduli (*G''*) as a measure for the viscous portion at an applied strain of 0.5. Expectedly, the pristine AZO surfactant behaves liquid-like as evidenced by the larger loss moduli (*G''*) compared to the storage moduli (*G'*) over the measured frequency range (0.1–20 Hz) (**Figure 3**A, black curve). When the nematic DNA–AZO samples were measured, typical LC viscoelasticity was observed by the emergence of a *G'* to *G''* crossover at 11 Hz (Figure 3A, blue curve and red curve). We attribute the increased elastic moduli of the DNA–AZO mesophases, as compared to the pristine AZO surfactant, to the additionally introduced DNA backbone. Notably, when backbone rigidity increased from ssDNA to helical dsDNA the stiffness of the TLC materials was enhanced and viscosity increased significantly (Figure 3B). The mechanical properties of the complexes comprising *Z*-isomer could not be investigated employing shear rheometry as most likely penetration depth of UV-light into thin films is not sufficient to change the bulk mechanical properties of the sample sufficiently to be detectable beyond the error of measurement.

Therefore, we investigated the photoresponsive mechanical properties of the TLC materials employing AFM-based nanoindentation.[62,63] Three thin films including pristine AZO surfactant, dsDNA–AZO, and ssDNA–AZO were prepared by drop-casting and deposited on Si substrates. First, the pristine film of AZO surfactant was investigated. Upon UV-irradiation (λ_{exc} = 365 nm, 3.6 mW cm^{-2} for 15 min) alteration of the surface topography was observed by AFM imaging (**Figure 4**). Concomitantly, the stiffness of the material decreased significantly. Notably, no heating of the film sample was noticed while irradiating our setup.[64]
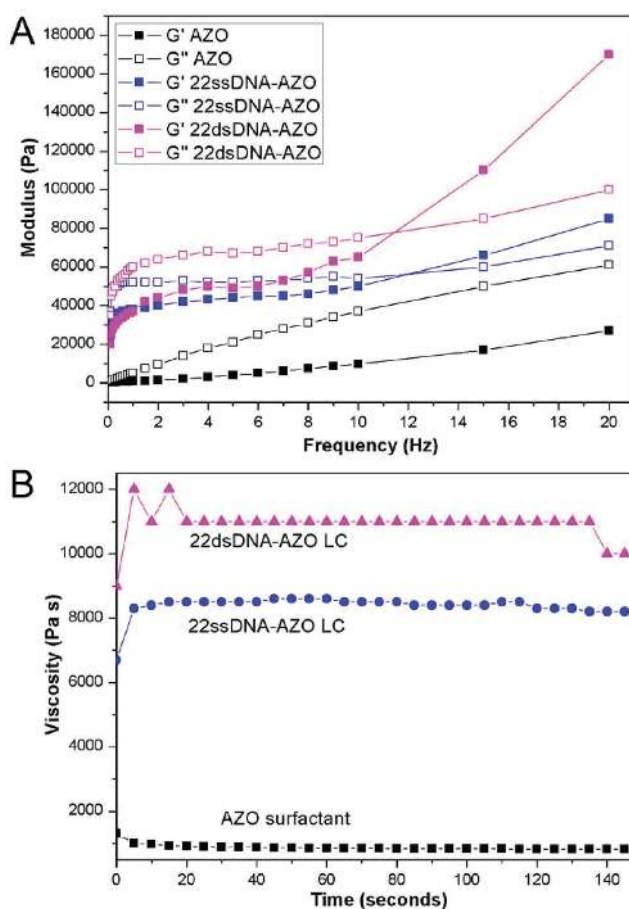

Figure 3. Dynamic mechanical analysis of the TLC materials employing a shear rheometer. A) Storage (*G'*) and loss (*G''*) moduli as function of shear frequency of the AZO surfactant (black curve), the dsDNA–AZO (pink curve), and the ssDNA–AZO (blue curve) complexes (strain = 50%, *T* = 25 °C) and B) corresponding viscosity measurement at *f* = 1 Hz (strain = 50%, *T* = 25 °C).

The observed effect thus indicates that the *E*- to *Z*-isomerization of the azobenzene moiety can alter the stiffness of the surfactant in the film.

Next, AFM measurements on the dsDNA–AZO sample were carried out and revealed notable changes in the mechanical characteristics over the course of irradiation with UV light. Before UV exposure, the sample surface was heterogeneous with an elastic constant varying between 1.4 and 12.0 N m^{-1} (**Figure 5**). However, after the samples were irradiated with UV-light, a surprisingly homogeneous stiffness of the same surface with an elastic constant of 1.6 ± 0.5 N m^{-1} (mean ± s.d.) was measured. The film also became more soft as evidenced by the absence of break-through events in the force–distance (*F–D*) curve (Figure 5B,E). Control experiments involving the ssDNA–AZO film indicate no apparent difference in stiffness before and after UV-irradiation for these films (Figure S16, Supporting Information). These results suggest that photoswitching of the azobenzene moiety in the dsDNA–AZO complex might induce a structural change large enough to be reflected in the macroscopic properties of the material. Interestingly while the pristine films of AZO surfactant show a large change in surface roughness
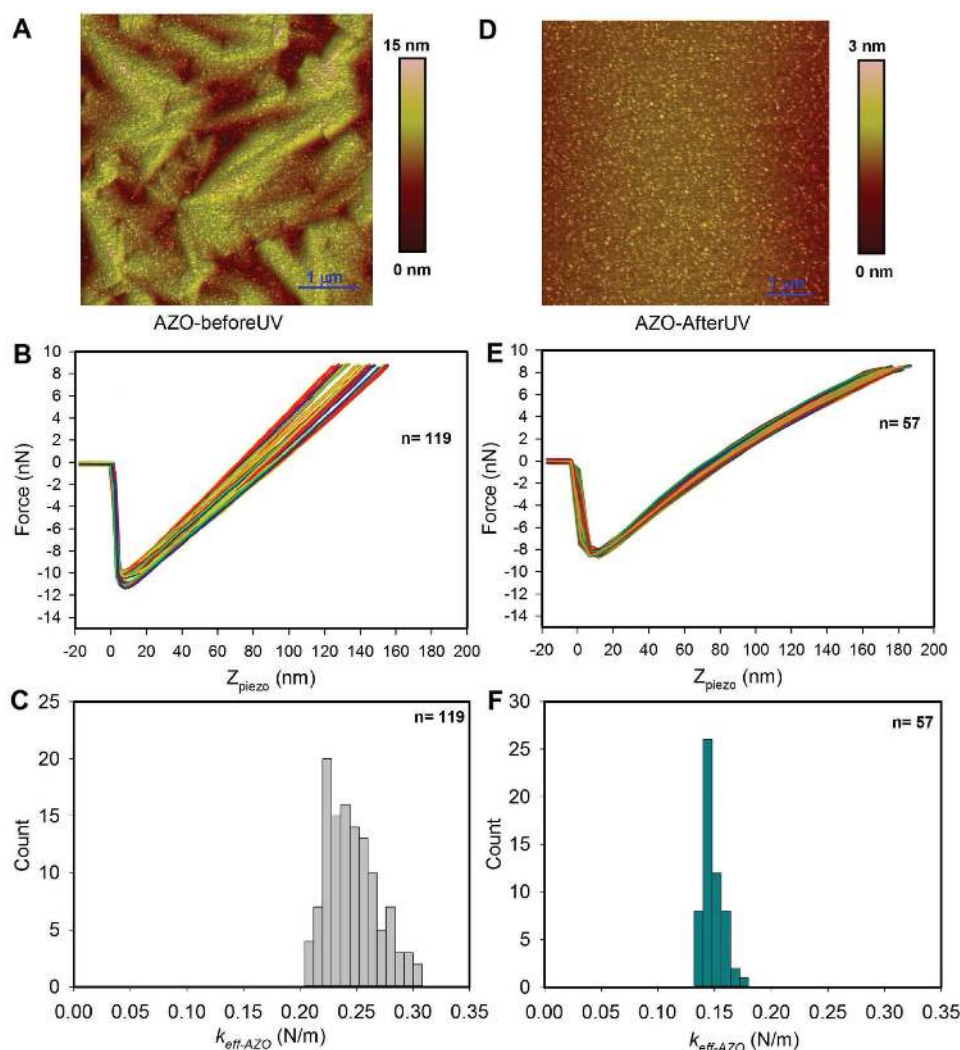
Figure 4. AFM-based nanoindentation on a thin film of the AZO surfactant. A) Surface topography of the film before UV-irradiation with height differences of around 13 nm. B) Superposition of F–D curves taken from the surface in panel A. C) Histogram of calculated spring constant of the AZO thin film from the F–D curves in panel B, measured $k_{eff-AZO} = 0.24 \pm 0.03$ N m^{-1} (mean ± s.d.). D) Surface topography of the film after irradiation with UV-light ($\lambda_{exc} = 365$ nm, 3.6 mW cm^{-2}, 15 min). The measured height differences decreased to around 2 nm. E) Superposition of F–D curves taken from the surface in panel D. F) Histogram of calculated spring constant of the AZO thin film from the F–D curves in E, measured $k_{eff-AZO} = 0.15 \pm 0.01$ N m^{-1}.

after UV irradiation, this change is absent in the dsDNA–AZO and ssDNA–AZO TLC materials.

3. Conclusions

A structurally novel azobenzene surfactant containing a quaternary ammonium group and two alkyl chains was successfully synthesized. The pristine surfactant material forms a broad mesophase with a layered structure. Once it is complexed with DNA, photoresponsive nucleic acid-based TLCs are obtained. In stark contrast to the pristine surfactant, a nematic mesophase over a broad temperature range from −7 to 110 °C was detected. The hybridization state of double stranded DNA is preserved in the TLCs at room temperature. The viscoelastic properties (elastic moduli and viscosity) of the DNA–AZO complexes correlate with the structure of DNA. In comparison to previous reports[33,38] involving

smectic DNA TLCs containing another type of surfactant, which lacks an aromatic moiety, we conclude that the introduction of an appropriate surfactant is important to modulate the mesophase structure and mechanical performance of the resulting complexes. Remarkably, upon irradiation with UV-light, the E- to Z-isomerization of the azobenzene moiety was successfully realized in the solvent-free DNA-AZO TLC materials. Concomitantly, photoresponsive mechanical manipulation could be achieved, whereby the stiffness of the TLC materials is in general smaller after the treatment with UV light. The characteristics of DNA fluidity and stimuli-responsive mechanical behavior might allow the development of DNA-based smart materials by further exploiting their recognition or self-healing properties. Furthermore, it should be mentioned that unspecific photodegradadtion of the AZO moiety exists in the TLC systems. Thus, optimization of the electronic properties of the AZO molecules to improve their photostability will play an important
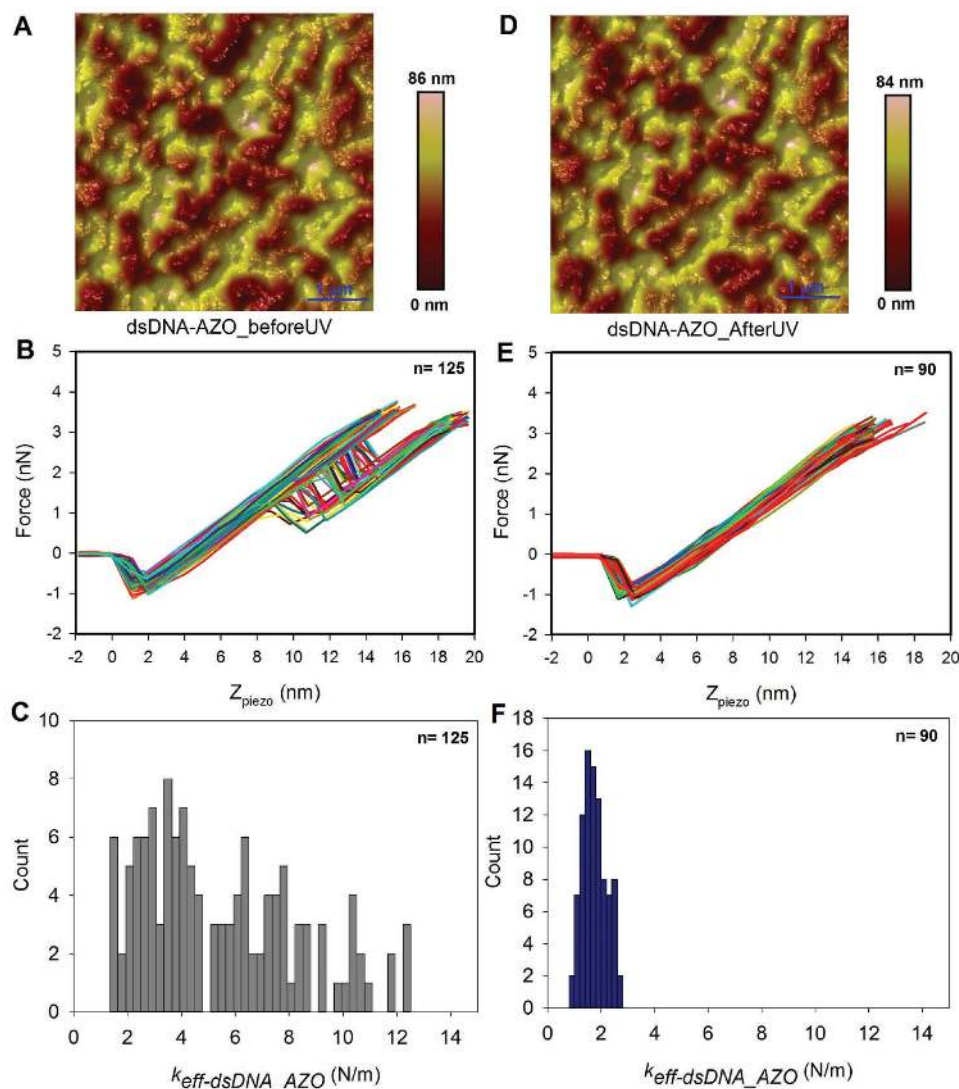
Figure 5. AFM-based nanoindentation on a thin film of the dsDNA–AZO complex. A) Surface topography of the film before irradiation with UV-light, with height differences of around 65 nm. B) Superposition of *F–D* curves taken from the surface in panel A. C) Histogram of calculated spring constant of the dsDNA–AZO thin film from the *F–D* curves in panel B with. The calculated spring constant is highly variable from 1.4 to 12.0 N m^{-1}. D) Surface topography of the film after the application of UV-light (λ_{exc} = 365 nm, 3.6 mW cm^{-2}, 15 min). The measured height differences is around 65 nm. E) Superposition of *F–D* curves taken from the surface in panel D. F) Histogram of calculated spring constant of the dsDNA–AZO film from the *F–D* curves in (E), $k_{eff\text{-}dsDNA\text{-}AZO}$ = 1.6 ± 0.5 N m^{-1} (mean ± s.d.).

role to expand multifunctionality and practical applications of DNA–AZO TLC materials.

4. Experimental Section

Materials: 4-Octyaniline, phenol, 2,4-dihydroxybenzoic acid, 1-bromobutane, 1,4-dibromobutane, *N,N′*-dicyclohexyl-carbodiimide (99%), 4-dimethylaminopyridine (99%), and trimethylamine solution (4.2 M) were obtained from Sigma-Aldrich. All the starting compounds for the synthesis of AZO surfactant were used without further purification. All solvents and reagents for oligonucleotide synthesis were purchased from Sigma-Aldrich and Novabiochem (UK). Solid supports (Primer SupportTM, 200 µmol g^{-1}) from GE Healthcare were used for the synthesis of DNA. 3-Hydroxypicolinic acid was employed as matrix during mass

spectrometry. Ultrapure water with a resistivity of ≈18.2 MΩ cm was used for all experiments. Other solvents used in the work were analytical grade.

Synthesis of AZO Surfactant: The cationic surfactant containing an azobenzene unit was synthesized in six steps (synthesis details in the Supporting Information). The synthesis route was inspired by procedures described for similar azobenzene derivatives.[52]

Synthesis of Oligonucleotides: 22mer oligonucleotide with a sequence 5′-CCTCGCTCTGCTAATCCTGTTA-3′ and its complementary sequence 5′-TAACAGGATTAGCAGAGCGAGG-3′ were synthesized using standard automated solid-phase phosphoramidite coupling methods[56] on an ÄKTA oligopilot plus (GE Healthcare) DNA synthesizer.

Preparation of DNA–AZO Complexes: First, DNA hybridization was carried out in an aqueous buffer solution (10 × 10^{-3} M MgCl$_2$, 50 × 10^{-3} M NaCl, and 10 × 10^{-3} M Tris–HCl, pH = 7.5) with a DNA

concentration of 2.4 mᴍ. The hybridized DNA solution was diluted by adding Milli-Q water. Thus, an aqueous solution of 22mer dsDNA with a concentration of ≈300 µm was obtained. In a second solution made from mixed water and ethanol (v/v = 5:3), the concentration of AZO surfactant was adjusted to $2-3 \times 10^{-3}$ ᴍ at room temperature. Both solutions were combined in a ratio so that ≈2 mol of surfactants equal 1 mol of phosphate group within DNA. After mixing aqueous solution of 22mer dsDNA with cationic AZO surfactant, a precipitate occurred. After centrifugation and lyophilization, the 22mer dsDNA–AZO complex was collected for further characterization. The 22mer ssDNA–AZO complex was prepared following the same procedures.

Additionally, a thin film of the 22mer dsDNA–AZO complex was fabricated by drop-casting for AFM based nanoindentation experiments. The lyophilized sample (1–2 mg) was dissolved in 30 µL CHCl₃. Then the solution was transferred to the smooth surface of a Si substrate (0.5 cm × 0.5 cm) by a pipette. After drying at ambient conditions for 48 hours, the film of the 22mer dsDNA–AZO complex was formed. Thin films of the 22mer ssDNA–AZO complex and pristine AZO surfactant were prepared following the same procedures.

Characterization: UV–Vis spectra were measured on a JASCO V-630. FT-IR spectra were recorded by a Bruker IFS88 instrument. NMR spectra were measured on a Varian Mercury NMR spectrometer at 25 °C (400 MHz for ¹H-NMR; 100 MHz for ¹³C-NMR). Liquid chromatography–mass spectrometry (LC–MS) analysis was performed on a Waters Xevo G2 UPLC/TOF. DNA sequences were purified by high-performance liquid chromatography (ÄKTA DNA explorer, GE Healthcare). Mass spectrometric analysis was performed using a 4800 MALDI-TOF/TOF Analyzer. POM was conducted on a Zeiss Axiophot. TGA was carried out using a TA Instruments Q1000 system in a nitrogen atmosphere and with a heating/cooling rate of 10 °C min⁻¹. SAXS was performed by employing a conventional X-ray source with radiation wavelength of $\lambda = 1.54$ Å and a Bruker Nano/microstar machine was used to obtain small angle scattering profiles, where the sample-to-detector distance was 24 cm. The sample holder is a metal plate with a small hole (diameter ≈0.25 cm, thickness ≈0.15 cm), where the X-ray beam passes through. The scattering vector q is defined as $q = 4\pi \sin\theta/\lambda$ with 2θ being the scattering angle. Rheology was investigated by a shear strain controlled Bohlin VOR rheometer (Bohlin Reologi AB) with two stainless steel fixtures.[65]

AFM based nanoindentation experiments were carried out on a Bruker Multimode AFM using Bruker SNL-A cantilevers with a nominal spring constant $k_{cantilever}$ of 0.35 N m⁻¹. The $F-D$ curves were recorded at a tip velocity of 1 µm s⁻¹. A variety of approaches are reported in literature to determine surface material properties. Analyzing the force–distance curves on the AZO and DNA–AZO surfaces it turns out that the force response is roughly linear. Therefore we have chosen to use Hooke's law for two springs in series to characterize the material properties of the films, yielding an effective elastic constant k_{eff} of the films. This approach is particularly suitable for comparison of the material properties of the same film before and after the application of UV light irradiation.

Supporting Information

Supporting Information is available from the Wiley Online Library or from the author.

Conflict of Interest

The authors declare no conflict of interest.

[1] F. Livolant, *Physica A* **1991**, *176*, 117.
[2] H. H. Strey, R. Podgornik, D. C. Rau, V. A. Parsegian, *Curr. Opin. Struct. Biol.* **1998**, *8*, 309.
[3] T. Bellini, R. Cerbino, G. Zanchetta, *Top Curr. Chem.* **2012**, *318*, 225.
[4] T. E. Strzelecka, M. W. Davidson, R. L. Rill, *Nature* **1988**, *331*, 457.
[5] F. Livolant, A. M. Levelut, J. Doucet, J. P. Benoit, *Nature* **1989**, *339*, 724.
[6] H. H. Strey, J. Wang, R. Podgornik, A. Rupprecht, L. Lu, V. A. Parsegian, E. B. Sirota, *Phys. Rev. Lett.* **2000**, *84*, 3105.
[7] J. Pelta, D. Durand, J. Doucet, F. Livolant, *Biophys. J.* **1996**, *71*, 48.
[8] F. Livolant, A. Leforestier, *Prog. Polym. Sci.* **1996**, *21*, 1115.
[9] L. Dai, Y. Mu, L. Nordenskiöld, A. Lapp, J. R. C. van der Maarel, *Biophys. J.* **2007**, *92*, 947.
[10] M. Nakata, G. Zanchetta, B. D. Chapman, C. D. Jones, J. O. Cross, R. Pindak, T. Bellini, N. A. Clark, *Science* **2007**, *318*, 1276.
[11] G. Zanchetta, M. Nakata, M. Buscaglia, T. Bellini, N. A. Clark, *Proc. Natl. Acad. Sci. USA* **2008**, *105*, 1111.
[12] T. Bellini, G. Zanchetta, T. P. Fraccia, R. Cerbino, E. Tsai, G. P. Smith, M. J. Moran, D. M. Walba, N. A. Clark, *Proc. Natl. Acad. Sci. USA* **2011**, *109*, 1110.
[13] G. Zanchetta, F. Giavazzi, M. Nakata, M. Buscaglia, R. Cerbino, N. A. Clark, T. Bellini, *Proc. Natl. Acad. Sci. USA* **2010**, *107*, 17497.
[14] M. Salamonczyk, J. Zhang, G. Portale, C. Zhu, E. Kentzinger, J. T. Gleeson, A. Jakli, C. De Michele, J. K. G. Dhont, S. Sprunt, E. Stiakakis, *Nat. Commun.* **2016**, *7*, 13358.
[15] T. P. Fraccia, G. P. Smith, G. Zanchetta, E. Paraboschi, Y. Yi, D. M. Walba, G. Dieci, N. A. Clark, T. Bellini, *Nat. Commun.* **2015**, *6*, 6424.
[16] J. O. Rädler, I. Koltover, T. Salditt, C. R. Safinya, *Science* **1997**, *275*, 810.
[17] I. Koltover, T. Salditt, J. O. Rädler, C. R. Safinya, *Science* **1998**, *281*, 78.
[18] K. K. Ewert, H. M. Evans, A. Zidovska, N. F. Bouxsein, A. Ahmad, C. R. Safinya, *J. Am. Chem. Soc.* **2006**, *128*, 3998.
[19] C. R. Safinya, J. Deek, R. Beck, J. B. Jones, C. Leal, K. K. Ewert, Y. Li, *Liq. Cryst.* **2013**, *40*, 1748.
[20] A. Zidovska, H. M. Evans, K. K. Ewert, J. Quispe, B. Carragher, C. S. Potter, C. R. Safinya, *J. Phys. Chem. B* **2009**, *113*, 3694.
[21] C. Leal, K. K. Ewert, N. F. Bouxsein, R. S. Shirazi, Y. Li, C. R. Safinya, *Soft Matter* **2013**, *9*, 795.
[22] N. F. Bouxsein, C. Leal, C. S. McAllister, K. K. Ewert, Y. Li, C. E. Samuel, C. R. Safinya, *J. Am. Chem. Soc.* **2011**, *133*, 7585.
[23] D. McLoughlin, M. Impéror-Clerc, D. Langevin, *ChemPhysChem* **2004**, *5*, 1619.

[24] C. Leal, A. Bilalov, B. Lindman, *J. Phys. Chem. B* **2009**, *113*, 9909.

[25] A. Bilalov, U. Olsson, B. Lindman, *Soft Matter* **2011**, *7*, 730.

[26] A. Krivtsov, A. Bilalov, U. Olsson, B. Lindman, *Langmuir* **2012**, *28*, 13698.

[27] G. Caracciolo, D. Pozzi, R. Caminiti, G. Mancini, P. Luciani, H. Amenitsch, *J. Am. Chem. Soc.*, **2007**, *129*, 10092.

[28] R. Dias, B. Lindman, *DNA Interactions with Polymers and Surfactants*, Weily-VCH, Weinheim, Germany **2008**.

[29] S. Chesnoy, L. Huang, *Annu. Rev. Biophys. Biomol. Struct.* **2000**, *29*, 27.

[30] K. R. Purdy Drew, L. K. Sanders, Z. W. Culumber, O. Zribi, G. C. L. Wong, *J. Am. Chem. Soc.* **2009**, *131*, 486.

[31] K. K. Ewert, A. Zidovska, A. Ahmad, N. F. Bouxsein, H. M. Evans, C. S. McAllister, C. E. Samuel, C. R. Safinya, *Top Curr. Chem.* **2010**, *296*, 191.

[32] N. W. Schmidt, F. Jin, R. Lande, T. Curk, W. Xian, C. Lee, L. Frasca, D. Frenkel, J. Dobnikar, M. Gilliet, G. C. L. Wong, *Nat. Mater.* **2015**, *14*, 696.

[33] K. Liu, D. Chen, A. Marcozzi, L. Zheng, J. Su, D. Pesce, W. Zajaczkowski, A. Kolbe, W. Pisula, K. Müllen, N. A. Clark, A. Herrmann, *Proc. Natl. Acad. Sci. USA* **2014**, *111*, 18596.

[34] Y. Okahata, T. Kobayashi, K. Tanaka, M. Shimomura, *J. Am. Chem. Soc.* **1998**, *120*, 6165.

[35] J. A. Hagen, W. Li, A. J. Steckl, J. G. Grote, *Appl. Phys. Lett.* **2006**, *88*, 171109.

[36] L. Cui, J. Miao, L. Zhu, *Macromolecules* **2006**, *39*, 2536.

[37] E. F. Gomez, V. Venkatraman, J. G. Grote, A. J. Steckl, *Adv. Mater.* **2015**, *27*, 7552.

[38] K. Liu, M. Shuai, D. Chen, M. Tuchband, J. Y. Gerasimov, J. Su, Q. Liu, W. Zajaczkowski, W. Pisula, K. Müllen, N. A. Clark, A. Herrmann, *Chem. Eur. J.* **2015**, *21*, 4898.

[39] L. Xu, M. Chen, J. Hao, *J. Phys. Chem. B* **2017**, *121*, 420.

[40] K. Liu, J. Varghese, J. Z. Gerasimov, A. O. Polyakov, M. Shuai, J. Su, D. Chen, W. Zajaczkowski, M. Marcozzi, W. Pisula, B. Noheda, T. T. M. Palstra, N. A. Clark, A. Herrmann, *Nat. Commun.* **2016**, *7*, 11476.

[41] M.-M. Russew, S. Hecht, *Adv. Mater.* **2010**, *22*, 3348.

[42] J. Zhang, Q. Zou, H. Tian, *Adv. Mater.* **2013**, *25*, 378.

[43] T. Ikeda, O. Tsutsumi, *Science* **1995**, *268*, 1873.

[44] T. J. White, D. J. Broer, *Nat. Mater.* **2015**, *14*, 1087.

[45] S. Iamsaard, S. J. Aßhoff, B. Matt, T. Kudernac, J. J. L. M. Cornelissen, S. P. Fletcher, N. Katsonis, *Nat. Chem.* **2014**, *6*, 229.

[46] T. Ikeda, J. Mamiya, Y. Yu, *Angew. Chem. Int. Ed.* **2007**, *46*, 506.

[47] L. T. de Haan, C. Sánchez-Somolinos, C. M. W. Bastiaansen, A. P. H. J. Schenning, D. J. Broer, *Angew. Chem. Int. Ed.* **2012**, *51*, 12469.

[48] M. Yamada, M. Kondo, J. Mamiya, Y. Yu, M. Kinoshita, C. J. Barrett, T. Ikeda, *Angew. Chem. Int. Ed.* **2008**, *47*, 4986.

[49] S.-K. Ahn, T. H. Ware, K. M. Lee, V. P. Tondiglia, T. J. White, *Adv. Funct. Mater.* **2016**, *26*, 5819.

[50] K. M. Lee, T. J. Bunning, T. J. White, *Adv. Mater.* **2012**, *24*, 2839.

[51] C. Li, Y. Liu, X. Huang, H. Jiang, *Adv. Funct. Mater.* **2012**, *22*, 5166.

[52] Y. Kamiya, H. Asanuma, *Acc. Chem. Res.* **2014**, *47*, 1663.

[53] Y. Yang, M. Endo, K. Hidaka, H. Sugiyama, *J. Am. Chem. Soc.* **2012**, *134*, 20645.

[54] A. Kuzyk, Y. Yang, X. Duan, S. Stoll, A. O. Govorov, H. Sugiyama, M. Endo, N. Liu, *Nat. Commun.* **2016**, *7*, 10591.

[55] W. Li, J. Zhang, B. Li, M. Zhang, L. Wu, *Chem. Commun.* **2009**, 5269.

[56] E. Merino, M. Ribagorda, *Beilstein J. Org. Chem.* **2012**, *8*, 1071.

[57] H. P. C. van Kuringen, Z. J. W. A. Leijten, A. H. Gelebart, D. J. Mulder, G. Portale, D. J. Broer, A. P. H. J. Schenning, *Macromolecules* **2015**, *48*, 4073.

[58] R. Klajn, *Pure Appl. Chem.* **2010**, *82*, 2247.

[59] F. E. Alemdaroglu, K. Ding, R. Berger, A. Herrmann, *Angew. Chem. Int. Ed.* **2006**, *45*, 4206.

[60] J. Zhou, S. K. Gregurick, S. Krueger, F. P. Schwarz, *Biophys. J.* **2006**, *90*, 544.

[61] T. Neumann, S. Gajria, M. Tirrell, L. Jaeger, *J. Am. Chem. Soc.* **2009**, *131*, 3440.

[62] W. H. Roos, R. Bruinsma, G. J. L. Wuite, *Nat. Phys.* **2010**, *6*, 733.

[63] J. Snijder, C. Uetrecht, R. J. Rose, R. Sanchez-Eugenia, G. A. Marti, J. Agirre, D. M. A. Guerin, G. J. L. Wuite, A. J. R. Heck, W. H. Roos, *Nat. Chem.* **2013**, *5*, 502.

[64] H. Zhou, C. Xue, P. Weis, Y. Suzuki, S. Huang, K. Koynov, G. K. Auernhammer, R. Berger, H. J. Butt, S. Wu, *Nat. Chem.* **2017**, *9*, 145.

[65] E. Polushkin, G. A. van Ekenstein, O. Ikkala, G. ten Brinke, *Rheol. Acta* **2004**, *43*, 364.